In Vivo Fluorescence of the Ocular Fundus Exhibits Retinal Pigment Epithelium Lipofuscin Characteristics

François C. Delori,† C. Kathleen Dorey,*† Giovanni Staurenghi,‡ Oliver Arend,§ Douglas G. Goger,* and John J. Weiter*†*

Purpose. To characterize the intrinsic fluorescence (autofluorescence) of the human ocular fundus with regard to its excitation and emission spectra, age relationship, retinal location, and topography, and to identify the dominant fluorophore among the fundus layers.

Methods. Using a novel fundus spectrophotometer, fluorescence measurements were made at 7° temporal to the fovea and at the fovea in 30 normal subjects and in 3 selected patients. Topographic measurements were made in 3 subjects. Ex vivo measurements of fluorescence of human retinal pigment epithelium (RPE) were obtained and compared to in vivo data.

Results. Fundus fluorescence reveals a broad band of emission between 500 and 750 nm, a maximum of approximately 630 nm, and optimal excitation of approximately 510 nm. Exhibiting a significant increase with age, this fluorescence is highest at 7° to 15° from the fovea, shows a well-defined foveal minimum, and decreases toward the periphery. In vivo fluorescence spectra are consistent with those obtained ex vivo on human RPE. Measurements with short wavelength excitation are strongly influenced by ocular media absorption and reveal an additional minor fluorophore in the fovea.

Conclusions. Spectral characteristics, correlation with age, topographic distribution, and retinal location between the choriocapillaris and the photoreceptors suggest that the dominant fundus fluorophore is RPE lipofuscin. The minor fluorophore is probably in the neurosensory retina but has not been identified. Invest Ophthalmol Vis Sci. 1995;36:718–729.

Lipofuscin is an autofluorescent pigment that accumulates in the lysosomes of most aging eukaryotic cells. Intensively studied as a biomarker for cellular aging and as a cumulative index of oxidative damage, mounting evidence across the biologic spectrum indicates that lipofuscin may play an important role in cellular aging and disease.

In the human retinal pigment epithelium (RPE), lipofuscin accumulates as a byproduct of phagocytosis of photoreceptor outer segments. In advanced age, lipofuscin is a major constituent of the RPE cell because it may occupy 20% of the free cytoplasmic space of the cell.[1] It has been postulated that excessive levels of lipofuscin in the RPE could compromise its essential functions and that lipofuscin contributes to the pathogenesis of age-related macular degeneration (ARMD).[1–8] The concept that lipofuscin may impair essential RPE functions is supported by the observations that elevated levels of lipofuscin are associated with decreased numbers of photoreceptors in humans.[9] The spatial topography, age relationship, and racial distributions of lipofuscin exhibit remarkable similarity to patterns seen in ARMD (summarized by Dorey et al[3]). Loss of visual function in inherited diseases such as Stargardt's disease[10] and Batten's disease (ceroid lipofuscinosis)[11] also has been attributed to excessive accumulation of lipofuscin-like materials in the RPE. The biologic significance of lipofuscin remains controversial because most of the evidence is circumstantial, having been obtained from dead tissue in which the temporal information is lost. A means for noninvasive measurement of lipofuscin in vivo is essential to resolve these questions.

*From the *Macular Degeneration Research Center, The Schepens Eye Research Institute, Boston; †Department of Ophthalmology, Harvard Medical School, Boston, Massachusetts; ‡Clinica Oculista, Ospedale San Paolo, Milan, Italy; and §Augen Klinic, Rheinisch–Westfälische Technische Hochschule, Aachen, Germany.*
Presented in part at the annual meeting of the Association for Research in Vision and Ophthalmology, Sarasota, Florida, 1993.
Supported by National Institute of Health grant EY08511 (FCD, CKD, JJW) and in part by NIH grant EY08121 (CKD), by Deutsche Forschungsgemeinschaft Ar 197/4-1 (OA), and by the Hearst Foundation, New York, New York (FCD, CKD).
Submitted for publication June 22, 1994; revised September 20, 1994; accepted October 7, 1994.
Proprietary interest category: N.
Reprint requests: François Delori, Schepens Eye Research Institute, 20 Staniford Street, Boston, MA 02114.

Investigative Ophthalmology & Visual Science, March 1995, Vol. 36, No. 3

Although it is routinely excited by ultraviolet light, lipofuscin has a broad range of excitation, from 300 to 500 nm.[4] The ability to excite lipofuscin with visible light made it feasible to elicit this fluorescence in vivo. We have developed a novel fundus spectrophotometer for noninvasive measurement of intrinsic fluorescence of the ocular fundus.[12,13] Our technique allows for the determination of fluorescence excitation and emission spectra from discrete sites of the fundus. We have shown that although the absolute fundus fluorescence measurement is affected by lens absorption, it is minimally influenced by the strong fluorescence of the crystalline lens.[13] We have also demonstrated that detailed spectral information is attainable with our method, which is essential in identifying the nature of the fluorophores and understanding the influence of other ocular pigments. In this article, we demonstrate that the dominant fluorophore detected noninvasively exhibits the spectra, topographic distribution, age relationship, and retinal location of RPE lipofuscin.

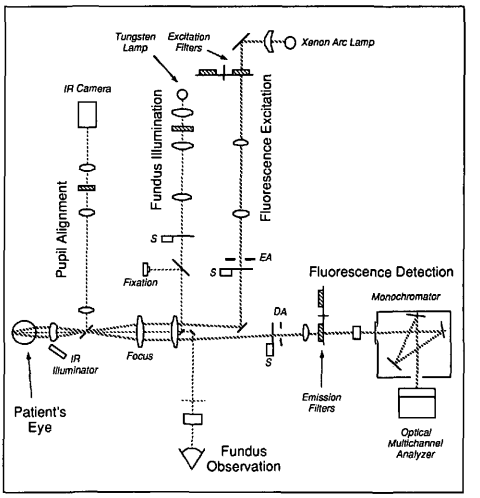

FIGURE 1. Optical diagram of the fundus spectrophotometer. EA = confocal excitation; DA = detection apertures; S = shutters; IR = infrared.

METHODS

Subjects

The study population included 30 subjects between 21 and 67 years of age (6 per decade, 14 women and 16 men). All subjects were white, had no fundus pathology, and had no or minimal nuclear sclerosis. In addition, we measured the fluorescence in three patients with selected pathology to help localize the fundus fluorophores. One patient was a 60-year-old woman with full-thickness, longstanding, macular hole (stage 3,[14] no neurosensory retina) in one eye and a normal fellow eye. The macular hole had a diameter of 400 μ and was surrounded by a distinct whitish cuff of about 600 μ in diameter. The second patient was a 70-year-old woman with ARMD and extended atrophy (few remaining RPE cells). The third patient was a 50-year-old woman with Stargardt's disease (in which histologic sections display dramatic increases in lipofuscin-like material in RPE lysosomes[10]). Fluorescein angiography demonstrated the dark choroid sign but no evidence of obvious atrophy. Visual acuity was 20/20 in both eyes.

The tenets of the Declaration of Helsinki were followed, informed consent was obtained for all subjects, and Institutional Human Experimentation Committee approval was granted. The pupil of one eye was dilated to a diameter of at least 6.5 mm with 1% tropicamide.

Fundus Spectrophotometer

Intrinsic fundus fluorescence was characterized using our fundus spectrophotometer. The technique, described in detail elsewhere,[13] allows measurement of fluorescence spectra from discrete sites on the fundus within 35° of the fovea.

A simplified diagram of the instrument is presented in Figure 1. Fluorescence excitation was derived from a xenon arc lamp, and interference excitation filters were centered at 430, 450, 470, 490, 510, 530, and 550 nm (full width at half maximum [FWHM] = 20 nm). The excitation field was defined by aperture EA and corresponded to a 3° diameter retinal field. The exposure duration for each excitation was 180 msec, and retinal radiant exposures were between 10 and 17 mJ/cm^2. The fluorescent and reflected light were collected by aperture DA that defined a 2° (585 μ) diameter sampling field on the retina (centered in the excitation field). Reflected light was rejected by high-pass emission filters, and the fluorescence—after dispersion by a monochromator and amplification by a cooled image intensifier—was spectrally analyzed by an optical multichannel analyzer (OMA, EGG-PAR Instruments, Bedford, MA). Fluorescence was integrated simultaneously in 512 wavelength channels in the spectral range 360 to 900 nm with an effective spectral resolution of 6 nm.

The subject's pupil was aligned under infrared illumination, and the site of interest was selected while the operator viewed the fundus (540 to 620 nm light); the subject's gaze was directed with an internal fixation target (668 nm). Accurate focus was achieved by concentrically aligning images of the excitation and the sampling fields on the subject's fundus.[18] The fluorescence spectrum measurement at each excitation wavelength was followed by a baseline spectrum mea-

surement to account for contributions of lens fluorescence scattered within the lens, stray fluorescence in the instrument, and dark–leakage current from the detector.[13] All light levels used for excitation, illumination, and focusing are within the safety limits recommended by the American National Standards Institute.[13,15]

Fundus Fluorescence Measurements

For all subjects, we used a sampling area of 2° to characterize fundus fluorescence at two sites: at 7° temporal to the fovea (7° temporal) and at the fovea. At each site, we measured emission spectra for excitation wavelengths of 430, 470, 510, and 550 nm. In selected subjects, we also used the intermediate wavelengths of 450, 490, and 530 nm. A single spectrum was recorded for all excitation wavelengths, except for 510 nm, at which two spectra were recorded at each site. Topographic distribution of the fluorescence was measured in three subjects along a horizontal line through the fovea for a range 30° nasal to 30° temporal to the fovea (2° field at ≈3° intervals) using an external fixation target to adjust retinal position.

Analysis

Fundus fluorescence $\Phi(\Lambda,\lambda)$ is defined as the spectral radiant energy emitted at an emission wavelength λ in a solid angle of 1 steradian (sr), for an excitation energy of 1 J at the excitation wavelength Λ. Units for $\Phi(\Lambda,\lambda)$ are $nJ \cdot nm^{-1} \cdot sr^{-1}/J$.

The fluorescence intensity $\Phi(\Lambda,\lambda)$ is calculated from the optical multichannel analyzer signal (OMA_λ in counts·pixel^{-1}) and its baseline ($OMA_{\lambda,bas}$), accounting for the spectral characteristics of the detector, filters, and optical system, using[13]:

$$\Phi(\Lambda,\lambda) = K_{opt} \cdot n^2 \cdot f_e^2 \cdot \frac{(OMA_\lambda - OMA_{\lambda,bas})}{G \cdot Q_{ex,\Lambda} \cdot T_{b,\lambda} \cdot S_\lambda} \quad (1)$$

where K_{opt} = 95.5 pixel·cm^{-2}·sr^{-1}·nm^{-1} is an instrument factor, n the refractive index of the vitreous (n = 1.336), f_e the anterior focal length of the eye assumed to be emmetropic (f_e = 1.68 cm), G the gain of the image intensifier, $Q_{ex,\Lambda}$ the energy (J) entering the eye for excitation wavelength Λ, $T_{b,\lambda}$ the transmission of the blocking filter at λ, and S_λ the spectral sensitivity of the detecting system at λ for G = 1 (OMA counts.J^{-1}). The energies $Q_{ex,\Lambda}$ and the spectra $T_{b,\lambda}$, and S_λ were obtained from system calibration. In this article, we have not accounted for the transmission losses of the ocular media.[16] Therefore, all fluorescence intensities $\Phi(\Lambda,\lambda)$ include transmission factors for the media at Λ and at λ.

The frequently used measure for fundus fluorescence, $\Phi(510, 620)$, was derived by averaging the spectral data in a 20-nm band centered at 620 nm. Results for the two measurements at Λ = 510 nm were averaged. For all subjects, the coefficient of variation associated with these two measurements was 2.5% on average at 7° temporal (range, 0.08% to 15%) and 3.2% on average at the fovea (range, 0.05% to 23%).

Excitation spectra were obtained by plotting the fluorescence intensity at λ = 620 nm as a function of the excitation wavelength Λ, that is, $\Phi(\Lambda,620)$. Emission maxima were determined by a 50 nm wide parabolic fit around the maximum. The widths of the emission spectra were expressed by the FWHM.

Ex Vivo Measurements

In vivo spectra were compared to spectra obtained from flat preparations of human RPE. Four donor eyes (donor ages, 60, 63, 64, and 72 years) were fixed in 4% paraformaldehyde in 0.1 M cacodylate buffer (pH, 7.2 to 7.4) for several hours and stored in phosphate buffer. After removing the anterior segment and vitreous, specimens were punched (7 mm diameter) from a site centered at 8 to 10 mm temporal to the fovea (26° to 33°). The macular tissue was used in other studies. Fluorescence measurements were made from the center of the punched area using all excitation wavelengths. Ex vivo fluorescence was also evaluated for a flat mount of unfixed RPE and choroid from a 65-year-old donor. Fluorescence measurements were made from two sites at approximately 5 mm from the fovea (about 16°). All ex vivo measurements were performed with the same exposure time and filters used in vivo. The preparations were located at the focal plane of a 36.5-mm lens placed in front of the fundus spectrometer. Equation (1) is used with f_e = 36.5 mm and n = 1.

RESULTS

Intrinsic Fluorescence in Individual Subjects

Representative fluorescence spectra measured in two individuals (ages, 23 and 62 years) at 7° temporal and at the fovea are shown in Figure 2. Fundus fluorescence is emitted across a broad band (500 to 800 nm) with a maximum at 620 to 640 nm, and optimal excitation occurs for Λ = 510 nm excitation. The emission spectra at 7° temporal (Fig. 2, top) have approximately the same shape for different excitation Λ, indicating the predominance of a fluorophore with peak emission at approximately 630 nm. Fluorescence at the fovea is considerably lower than at 7° temporal in both subjects, especially for short excitation wavelengths as demonstrated by the differences in the shape of the excitation spectra at the fovea and at 7° temporal (Fig. 2). The foveal emission spectra obtained with long excitation wavelengths (Λ = 510 and 550 nm) have shapes similar to those seen at 7° temporal. With short wavelength excitations (Λ = 430 and 470 nm) the

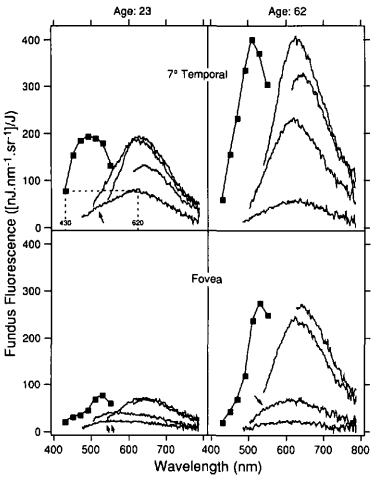

FIGURE 2. Fluorescence spectra measured at 7° temporal to the fovea (*top*) and at the fovea (*bottom*) in two normal subjects, ages 23 (*left*) and 62 (*right*) years. Sampling field, 2°. In each panel, the continuous curves are emission spectra for the excitation wavelengths 430, 470, 510, and 550 nm, and solid squares connected by a line is the excitation spectrum for fluorescence emission at 620 nm. The interrupted line (upper left, for $\Phi(430,620)$) illustrates how the excitation spectrum is related to the emission spectra. Emission spectra for 450, 490, and 530 nm excitation were omitted for clarity. (*arrows*) Spectral distortions caused by the minor fluorophore.

shapes are different, particularly in the young subject (Fig. 2, bottom left) in whom the spectra exhibit a broad maximum in the 520 to 580 nm spectral range (double arrows), suggesting that another fluorophore is being excited in that spectral range. Subtle distortions seen on other spectra (single arrows) are also consistent with added fluorescence from a minor fluorophore.

Age Dependence

Figure 3 illustrates the age-related increase of $\Phi(510,620)$ at 7° temporal and at the fovea for all normal subjects in the study. Table 1 gives the average $\Phi(\Lambda,620)$ for different Λ and sites, as well as the correlations with age. The increase in fundus fluorescence with age is highly significant at both sites when $\Lambda >$ 470 nm. Fluorescence excited at Λ = 470 nm correlates less strongly with age, and no correlation is observed for Λ = 430 nm. This results from the effect of ocular media absorption: The age-related increase of fundus fluorescence, clearly seen with $\Lambda > 470$ nm, is canceled out by the age-related decrease in ocular media transmission at Λ = 430 nm. The short wavelength end of the excitation spectrum steepens substantially as age increases (Fig. 2). This is demonstrated by the very strong negative correlation of the ratio $\Phi(430,620)/\Phi(510,620)$ with age ($r = -0.93$, $P < 0.0001$).

Emission Maxima and Spectral Widths

Table 2 gives average values for the wavelengths of maximum emission (λ_{max}) and the spectral width (FWHM) for different excitation wavelengths Λ. The emission maximum shifts toward longer wavelengths, and the spectrum narrows as the excitation wavelength increases. The foveal spectra are broader than those at 7° temporal, and their λ_{max} occurs at shorter wavelengths for Λ = 430 and 470 nm and at slightly longer wavelengths for Λ = 510 and 550 nm.

Intersubject variability in λ_{max} and in spectral width, and hence in the shape of the spectra, is smallest when the fluorescence is intense (Λ = 510 nm) and highest when it is low (fovea, Λ = 430 and 470 nm). The broad emission maxima in the 520- to 580-nm spectral range, seen in Figure 2 (double arrows), are found for approximately one third of the foveal spectra (Λ = 430 and 470 nm), particularly when the fluorescence is low. Indeed, λ_{max} shifts significantly toward longer wavelengths when $\Phi(\Lambda,620)$ increases (for Λ = 430 nm: $r = +0.56$, $P = 0.0008$; for Λ = 470

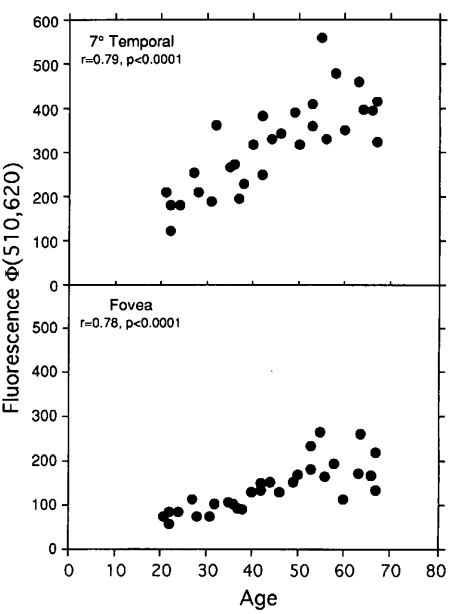

FIGURE 3. Fluorescence at 620 nm for excitation at Λ = 510 nm, $\Phi(510,620)$, for normal subjects (n = 30). (*top*) At 7° temporal to the fovea. (*bottom*) at the fovea. Sampling field, 2°.

TABLE 1. Fluorescence at 620 nm Obtained at 7° Temporal to the Fovea and at the Fovea Using Different Excitation Wavelengths (Λ)

	Excitation Wavelength Λ (nm)			
	Λ = 430	*Λ = 470*	*Λ = 510*	*Λ = 550*
Fluorescence at 7° temporal*	85 (21)	241 (24)	315 (33)	223 (41)
Correlation with age (r)	−0.14	+0.45	+0.79	+0.77
	$P = 0.45$	$P = 0.011$	$P < 0.0001$	$P < 0.0001$
Fluorescence at the fovea*	27 (34)	61 (37)	137 (41)	132 (51)
Correlation with age (r)	−0.08	+0.32	+0.78	+0.80
	$P = 0.65$	$P = 0.08$	$P < 0.0001$	$P < 0.0001$
Ratio of foveal to temporal fluorescence	0.32 (28)	0.25 (29)	0.43 (16)	0.59 (18)
Correlation with age (r)	−0.02	+0.07	+0.34	+0.42
	$P = 0.90$	$P = 0.72$	$P = 0.066$	$P = 0.019$

* Average fluorescence in $(nJ.nm^{-1}.sr^{-1})/J$ ($n = 30$ for all averages). All numbers in parentheses are coefficient of variation (in %).

nm: $r = +0.71$, $P < 0.0001$). These changes reflect the influence of a minor fluorophore at 520 to 580 nm: Its fluorescence only emerges above that of the dominant fluorophore when the fluorescence of the latter is low (Fig. 2). The emission spectra of this minor fluorophore (for Λ = 430 and 470 nm) can be estimated by comparing the foveal and temporal spectra: The difference spectra of Figure 4 (spectra A) reveal the emission spectra of the minor fluorophore with a maximum at 520 to 540 nm.

Topographic Distribution

The distribution of fundus fluorescence recorded along a horizontal line through the fovea (Fig. 5) shows a well-delineated minimum in fluorescence at the fovea, maximal fluorescence at 7° to 15° from the fovea, and a decrease in fluorescence toward the periphery. The optic disk fluoresces less intensely than does the surrounding retina, and it is characterized by different excitation and emission spectra,[13] indicating that a different fluorophore is involved.

The depth of the foveal minimum is more pronounced when shorter excitation wavelengths are used: The ratio of foveal fluorescence to temporal fluorescence is on average 0.59 at Λ = 550 nm, but it decreases to 0.25 at Λ = 470 nm (Table 1). If the excitation is attenuated by absorption of a pigment in the fovea, the difference spectrum $A(\Lambda) = \log \Phi(\Lambda,620)_{7^\circ\ temporal} - \log \Phi(\Lambda,620)_F$ should reflect the absorption spectrum of that pigment. The difference spectra (Fig. 6) are consistent with macular pigment absorption, indicating that excitation of the foveal fluorescence is attenuated by macular pigment (emission wavelengths are not affected because they occur outside the absorption range of macular pigment). In other words, the fluorophore must be located posterior to the macular pigment.

Bleaching Experiment

If fundus fluorescence originates from layers posterior to the photoreceptors, it should be affected by bleaching of photopigments. We tested this prediction by measuring the fluorescence (Λ = 450 nm) at 10° to 15° temporal to the fovea after a period of dark adaptation (15 minutes). Results for one 52-year-old subject (Fig. 7) show that bleaching occurs and that the difference spectrum between the light- and dark-adapted state, $A(\lambda) = \log \Phi(450,\lambda)_{LA} - \log \Phi(450,\lambda)_{DA}$, can

TABLE 2. Wavelengths of Maximum Emission λ_{max} and Full Width at Half Maximum

	Excitation Wavelength (nm)			
	Λ = 430	*Λ = 470*	*Λ = 510*	*Λ = 550*
λ_{max} (7° temporal)	620 ± 8	621 ± 6*	631 ± 4†	641 ± 6†
λ_{max} (fovea)	596 ± 29‡	603 ± 25*‡	634 ± 6†§	649 ± 8†§
FWHM (7° temporal)	209 ± 12	183 ± 6†	167 ± 4†	—
FWHM (fovea)	217 ± 15§	210 ± 15*§	182 ± 11†§	—

Averages ± SD in nm ($n = 30$, for all averages).
Comparisons by one-tailed paired *t*-tests: *greater than value on the left ($P < 0.05$; †greater than value on the left ($P < 0.0001$); ‡smaller than value above ($P < 0.001$); §higher than value above ($P < 0.001$).
FWHM = full width at half maximum.

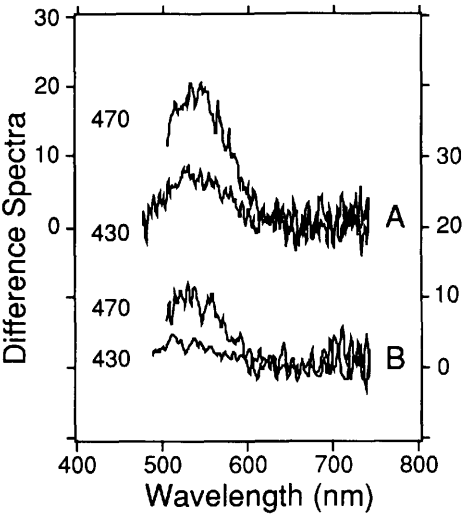

FIGURE 4. Estimated emission spectra of the minor fluorophore for excitation at Λ = 430 and 470 nm. (**A**) Younger normal subject in Figure 2. Difference spectra obtained by subtracting the scaled temporal spectra (Λ = 430 and 470 nm) from the corresponding foveal spectra (*left scale*). (**B**) Patient with uniocular macular hole (Fig. 9). Difference spectra obtained by subtracting the scaled spectra from the macular hole (Λ = 430 and 470 nm) from the corresponding foveal spectra of the fellow eye (*right scale*). In both patients, we assumed that the minor fluorophore did not substantially affect the long wavelengths (675 to 750 nm). The scaling was obtained by ensuring that the average of each difference spectrum between 675 and 750 nm was zero.

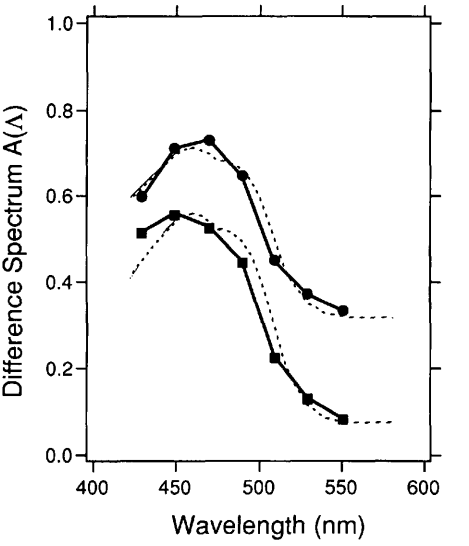

FIGURE 6. Difference spectra derived from the temporal (7° temporal) and foveal (F) excitation spectra for the 2 subjects of Figure 2: younger subject (*circles*) and older subject (*squares*). The difference spectrum is $A(\Lambda) = \log \Phi(\Lambda, 620)_{7^\circ \text{ temporal}} - \log \Phi(\Lambda,620)_F$. The interrupted lines are linear fits of the macular pigment absorption spectrum[44] to the experimental data. Macular pigment densities at 460 nm were found to be 0.42 and 0.51 for the younger and older subject, respectively (r^2 = 0.96 and 0.97).

be fitted to absorption spectrum of rhodopsin. Because the difference spectrum is the result of a double pass through rhodopsin (once at Λ and once at λ), one would expect the long wavelength plateau of A(700) to correspond with the effect of bleaching at the excitation wavelength (Λ = 450 nm). However, as shown in Figure 7, only part of A(700) can be accounted for by bleaching at 450 nm, indicating that another minor bleaching process is occurring. This experiment was repeated in two other subjects with similar results. For the three subjects (ages, 52, 42, and 32 years), the single-pass rhodopsin densities (at 500 nm) were 0.047 ± 0.002 (SD), 0.070 ± 0.003, and 0.047 ± 0.002 DU, respectively. The magnitude of the unexplained bleaching component x (Fig. 7) was 0.024 ± 0.002, 0.010 ± 0.003, and 0.023 ± 0.002 DU, respectively (r^2 if the linear fit were 0.83, 0.79, and 0.84, respectively).

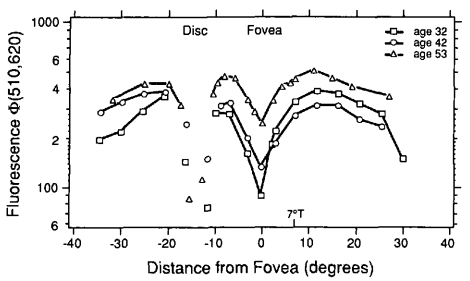

FIGURE 5. Topographic distribution of fundus fluorescence. Fluorescence $\Phi(510,620)$ in three subjects (ages, 32, 42, and 53 years) along a horizontal line through the fovea. Spatial resolution: 2°.

Ex Vivo Measurements

Figure 8 presents the comparison of emission spectra (Λ = 430, 470, and 510 nm) and excitation spectra obtained ex vivo from flat-mounted RPE of donor eyes to those from our in vivo measurements in the 10 oldest subjects of this study. The data for the four fixed retinas, for the unfixed retina, and for the 10 subjects were normalized and averaged. The spectral shape obtained for the unfixed sample (not shown in Fig. 8) did not differ substantially from that of the

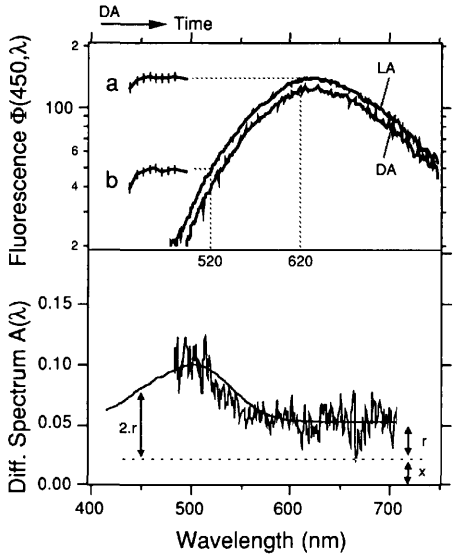

FIGURE 7. Effect of bleaching on the fluorescence at 10° to 15° temporal to the fovea (2° sampling field, Λ = 450 nm). (*top*) Dark-adapted (DA, first measurement) and light-adapted (LA) emission spectra in a 52-year-old subject. Curves a and b show the variation of fluorescence at 620 and 520 nm, respectively, for the successive measurements performed after dark adaptation (*vertical markers*). (*bottom*) Difference spectrum $A(\lambda) = \log \Phi(450,\lambda)_{LA} - \log \Phi(450,\lambda)_{DA}$. The smooth line is the linear fit (between 495 and 700 nm) of the rhodopsin spectrum[45] to the experimental data: Single-pass rhodopsin density at 500 nm was 0.047 DU (r^2 = 0.83). The long wavelength plateau A(700) can be decomposed into a component r due to rhodopsin bleaching at 450 nm, and a component x due to an additional minor bleaching process.

fixed tissue. The average fluorescence $\Phi(510,620)$ for the four fixed retinas, the unfixed tissue (two sites), and the 10 oldest subjects was 286 ± 43 (SD), 292 ± 92, and 408 ± 73 $(nJ \cdot nm^{-1} \cdot sr^{-1})/J$, respectively. The wavelength of maximal emission of the ex vivo spectra increases with Λ from 588 ± 7 nm at Λ = 430 nm to 610 ± 4 nm at Λ = 510 nm, similar to that observed in vivo, though at somewhat longer wavelengths (Table 2). The normalized ex vivo emission spectra are shifted toward shorter wavelengths (by approximately 10 to 25 nm) compared to the in vivo measured spectra. The normalized ex vivo excitation spectra are also shifted by approximately 30 to 50 nm toward shorter wavelengths compared to the in vivo spectra.

Selected Clinical Cases

Table 3 gives the fluorescence $\Phi(510,620)$ at 7° temporal and at the fovea for the selected clinical cases (subject ages, 50 to 70 years). For comparison, the average fluorescence and wavelengths are given for the 10 oldest normal subjects (mean age, 61 years). For the patient with macular degeneration, the fluorescence in atrophic areas was significantly lower than normal ($P < 0.0001$). The spectra had some signature of the dominant fluorophore but were very noisy and somewhat distorted. In the patient with Stargardt's disease, the fluorescence was significantly higher ($P < 0.0001$) than normal, and the spectra had essentially the same shape as those obtained in normal subjects.

A comparison of the normalized fluorescence spectra in the fovea in the two eyes of a patient with a uniocular macular hole is presented in Figure 9. Four distinct observations can be made: (1) For each

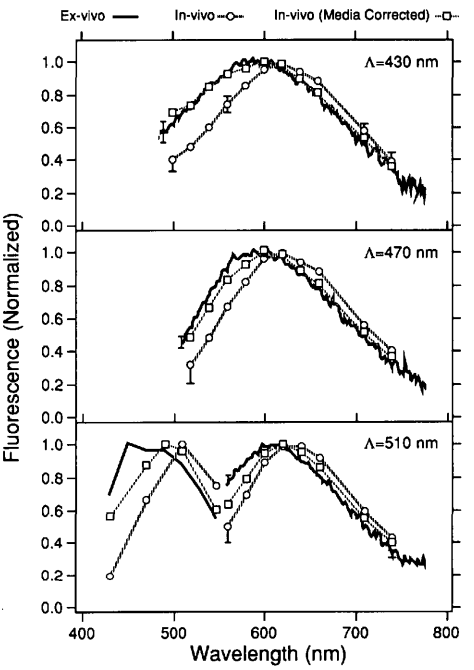

FIGURE 8. Comparison of ex vivo and in vivo fundus fluorescence. Normalized emission spectra obtained from donor eyes (*solid continuous lines*) and from in vivo measurements (*interrupted lines*) at excitation wavelengths Λ = 430, 470, and 510 nm (*top to bottom*). The ex vivo data are the average from four fixed donor eyes (donor ages, 60 to 72 years, *thick line*), and the in vivo data are the average from the 10 oldest subjects (mean age, 61 years, *open circles*). The open squares are the estimated spectra after correction for ocular media absorption (see Discussion). Error bars correspond to standard deviations of the normalized spectra. The bottom panel also contains the normalized excitation spectra $\Phi(\Lambda,620)$ corresponding to the same ex vivo and in vivo data (with identical symbols).

TABLE 3. Fluorescence Φ(510,620) at 7° Temporal to the Fovea and at the Fovea of Special Clinical Cases and Normal Control

	Fluorescence at 7° Temporal*	*Fluorescence* at the Fovea*
Normal eyes (10 oldest subjects)†	408 ± 73	187 ± 49
Eye with atrophy	72	48
Eye with Stargardt's disease (OS)	746	295
Eye with Stargardt's disease (OD)	629	442
Eye with macular hole (OS)	337	232
Normal fellow eye (OD)	339	128

* Fluorescence in $(nJ.nm^{-1}.sr^{-1})/J$. †Average ± SD.

Λ, the shape of the emission spectrum measured in the macular hole closely resembled that measured at 7° temporal, indicating that the dominant fluorophore detected at 7° temporal was the same as that detected when the neurosensory retina was absent. (2) The fluorescence Φ(510,620) was higher in the hole than at the fovea of the fellow eye (Table 3) because its excitation was not reduced by macular pigment absorption. This is confirmed by the fact that the excitation spectrum (Fig 9, bottom panel) at the macular hole was not distorted by the macular pigment absorption signature. (3) When excited at short wavelengths, the foveal emission spectrum of the normal fellow eye was broader and shifted toward shorter wavelengths. This is consistent with the presence of a minor short-wavelength fluorophore in the fovea of the fellow eye. Its emission spectra (for Λ = 430 and 470 nm) can be estimated by spectral subtraction of the foveal spectra of both eyes. The derived emission spectra of the minor fluorophore (Fig. 4, spectra B) had shapes similar to those obtained in the normal eye (spectra A), and they revealed a maximum emission at 520 to 540 nm. (4) The fact that the minor fluorophore was not seen in the macular hole indicated that it may have been located in the neurosensory retina.

DISCUSSION

Our results demonstrate that intrinsic fundus fluorescence results from at least two fluorophores—a dominant fluorophore with peak emission at 620 to 630 nm (optimal excitation at 510 nm) and a minor fluorophore with peak emission at 520 to 540 nm (optimal excitation at 430 to 470 nm). The minor fluorophore was best seen when the fluorescence of the dominant one was low, suggesting that these are indeed two fluorophores.

Dominant Fluorophore

The characteristics of the fundus fluorescence, including age relationship, topographic distribution, depth localization, and spectra, are all consistent with the hypothesis that the dominant fluorophore is RPE lipofuscin. Furthermore, results from selected clinical cases support this conclusion. In Stargardt's disease, in which the RPE contains large amounts of a lipofuscin-like material,[10] the fluorescence of the dominant fluorophore was substantially higher than normal, whereas in extended atrophy (ARMD), in which few RPE cells remain, the fluorescence was markedly decreased. Thus, although we cannot prove that the dominant fluorophore is lipofuscin, this is the simplest hypothesis consistent with the known facts.

Age Relation and Topographic Distribution. The age relationship and the topographic distribution of the

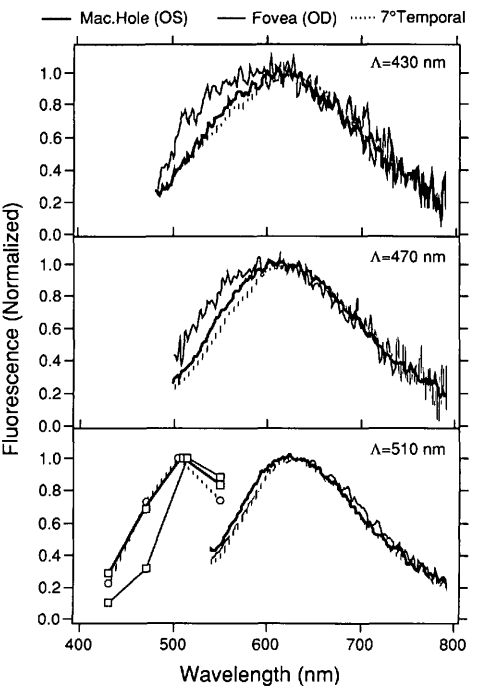

FIGURE 9. Fundus fluorescence from the patient with a unilocular, full-thickness macular hole. Excitation wavelengths Λ = 430, 470, and 510 nm (*top to bottom*). In each panel, normalized emission spectra from the macular hole (*solid thick line*), from the fovea in the fellow eye (*solid thin line*), and from 7° temporal (average for both eyes, *interrupted line*). Absolute values for Φ(510,620) are given in Table 3. The bottom panel also contains the normalized excitation spectra Φ(Λ,620) corresponding to the three sets of emission data (with same line symbols). For clarity, peak Λ were slightly displaced.

dominant fundus fluorophore are consistent with those of lipofuscin as measured in the RPE of human donor eyes. Ex vivo lipofuscin studies used measurements of fluorescence emitted from the RPE in section[7,17] and counts of the number of lipofuscin granules observed by electron microscope.[18]

The topographic distribution of fundus fluorescence (Fig. 5) is consistent with that of lipofuscin obtained in donor eyes[7,17,18]: It is highest at the posterior pole, there is a localized minimum at the fovea (of approximately 83%[7]), and it decreases toward the periphery. Because the foveal measurements are affected by macular pigment and by the high local concentration of RPE melanin, it is important to consider whether the decrease in foveal fluorescence is real or is a consequence of the measurement geometry. Macular pigment clearly contributes to the local minimum when excitation wavelengths within the absorption range of the macular pigment are used (Fig. 6, Table 1). However, the foveal minimum cannot be attributed entirely to absorption by macular pigment because foveal fluorescence excited at $\Lambda = 550$ nm, outside the macular pigment absorption range, still averages 59% of that at 7° temporal (Table 1). Similarly, RPE melanin absorption could lower the foveal fluorescence because it is denser at the fovea.[7,19] Using our previous data on RPE melanin densities,[7] and assuming that all melanin is located in the apical RPE cell, we estimate that melanin would lower the foveal fluorescence to 83% of the parafovea on average, not enough to account for the observed average decrease of 59%. Thus, even when the effects of macular pigment and RPE melanin are estimated, the foveal fluorescence remains low, which is consistent with the ex vivo observations.[7]

Localization Within the Fundus Layers. Reflectance spectra of the fundus[20,21] always reveal to various degrees the signature of absorption by choroidal blood because light penetrates into the choroidal layers. The fundus fluorescence emission spectra (Fig. 2) are continuous curves without a detectable signature of absorption by blood, that is, no sudden increase in fluorescence emission is observed above 580 nm, at which absorption by blood decreases rapidly.[22] In contrast, the fluorescence spectra from the optic disk[13] reveal a distinct blood absorption signature because the fluorescence emanates from within the capillary-filled disk tissue. Thus, the absence of the spectral signature of blood indicates that the fluorophore is located anterior to the choriocapillaris.

In contrast, the foveal fluorescence excitation spectra are affected by the spectral signature of the macular pigment (Fig. 6). Our macular pigment density estimates (0.42 and 0.51 DU) are consistent with densities obtained from psychophysical methods. Because the macular pigment is located in the superficial layers of the fovea,[23] this locates the fluorophore between the inner retina and the choriocapillaris.

Similarly, the fluorescence is affected by bleaching of rhodopsin. The difference spectra at approximately 500 nm are very noisy because the fundus fluorescence is low at these wavelengths. The rhodopsin densities (at 500 nm) at 10° to 15° temporal from the fovea calculated from our spectral fits (Fig. 7) in three subjects were between 0.045 and 0.075 DU (single pass). This is consistent with double-pass densities obtained by rod densitometry at 15° to 20° (maximum density of rods), that is, 0.15 to 0.20 DU (double pass).[24,25] Thus, the fluorescence of the dominant fluorophore is fully attenuated by the rods, and the fluorophore is therefore located posterior to the photoreceptor layer. The nature of the additional bleaching process detected in our experiment is not known and will require additional investigation to identify.

Finally, the evidence of the macular hole measurement parallels the other findings (Fig. 9, Table 3). Histopathologic studies have shown lack of neurosensory retinal tissues in patients with full-thickness macular holes, whereas the RPE complex remains intact.[26] Partial atrophy of the photoreceptors at the margin of the hole is present in most cases.[27] Our sampling field (585 μ diameter) included an area of exposed RPE (400 μ diameter, ~50% of sampling area) and a somewhat atrophic cuff of retina (600 μ diameter). If the dominant fluorophore were located primarily in the neurosensory retina, removal of at least half of the retina (fluorophore and macular pigment) would cause a strong decrease in fluorescence. Instead, we see an increase compared to the fellow eye (Table 3) because removal of macular pigment in the hole has exposed a fluorophore located posterior to the neurosensory retina.

Fluorescence Spectra. Comparison of the fluorescence spectra obtained in vivo with those from flat preparations of human RPE demonstrate good correspondence in the shape of the spectra but show a shift of the in vivo spectra toward longer wavelengths. This shift, in part, can be accounted for by increases in the ocular media transmission with wavelength throughout the visible spectrum.[28,29] We corrected the in vivo spectra to account for media absorption using the algorithm of Pokorny.[28] The corrected spectra (square in Fig. 8) show a better correspondence with those obtained ex vivo. However, ocular media absorption only partially accounts for the difference in the excitation spectra, probably because of the difficulties in accurately correcting for media absorption at the shortest excitation wavelengths.

Most published emission spectra have focused on chloroform methanol extracts of lipofuscin excited with ultraviolet light. These spectra demonstrate peak emission at approximately 570 to 590 nm, which is consistent with spectral measurements of emission

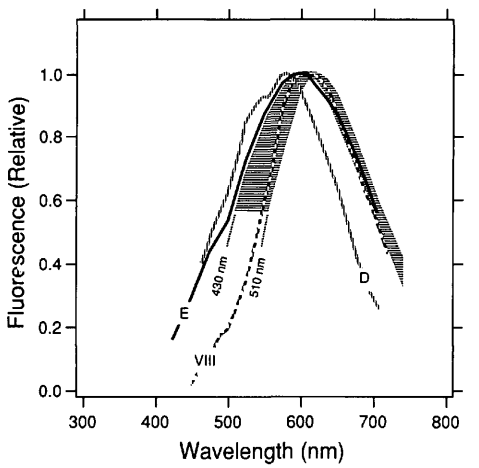

FIGURE 10. Comparison of in vivo fluorescence spectra and published lipofuscin spectra. Shaded area is the envelope of the in vivo emission spectra obtained with our excitation between Λ = 430 and 510 nm. These spectra incorporate a correction for ocular media absorption.[28] The other spectra are: E = emission spectrum (Λ = 340 nm) for a chloroform extract of a lipofuscin-laden human retinal pigment epithelium sample[4]; D = emission spectrum (Λ = 365 nm) from individual lipofuscin granules in paraffin sections of retinal pigment epithelium[31]; and VIII = emission spectrum (Λ = 420 nm) of one of the "orange-red" fluorophores separated by Eldred.[32]

from individual lipofuscin granules in paraffin sections of RPE.[30,31] As seen in Figure 10, the emission spectra obtained with 430 nm excitation in vivo exhibit good agreement with previous measurements of lipofuscin. However, when excited at 510 nm, the in vivo emission spectrum displays a marked shift toward longer wavelengths with maximum emission at ~630 nm. It is now known that lipofuscin is a mixture of at least 10 fluorophores, all of which are primarily excited in the ultraviolet range.[32] However, three of those lipofuscin fluorophores ("orange-red" emitters) have excitation spectra that extend substantially above 400 nm and dominant emission at 620 to 630 nm. The emission spectrum we obtained in vivo with 510 nm excitation indicates that this fluorescence may be predominantly derived from the group of orange-red fluorophores described by Eldred.[32,33]

Minor Fluorophores

The minor fluorophore (peak emission at 520 to 540 nm, Fig. 4) only substantially affects the fundus fluorescence if the fluorescence of lipofuscin is low, that is, at the fovea, at Λ < 510 nm, and for younger subjects. Its fluorescence then affects, to various degrees, the short wavelength side of the emission spectra and may cause—for very low lipofuscin—a broad maximum between 520 and 580 nm. Although it appears to be highest at the fovea, its presence may not be restricted to the fovea because traces of its signature may be seen in young subjects at 7° temporal with Λ = 430 nm (Fig. 2, top left). The fluorescence of the minor fluorophore does not appear to increase with age, as does the lipofuscin fluorescence, and its contribution appears negligible for Λ > 470 nm.

If the minor fluorophore is in the neurosensory retina, as suggested by the macular hole evidence, it could be FAD (flavin adenine dinucleotide, a component of the respiratory enzyme chain), the highest concentration of which is found in the mitochondria of the photoreceptor's inner segment. The fluorescence characteristics of FAD[34] (excitation peak, ≈460 nm; emission peak, ≈520 nm) are consistent with our observations. In attempting to demonstrate FAD fluorescence, Teich[35] used an excitation at 457 nm and reported changes in fundus fluorescence (500 to 700 nm) in one monkey with varying breathing conditions. However, no spectral identification of the FAD spectral signature was provided, and the work was not pursued. At this point, however, we cannot entirely exclude the possibility that the minor fluorophore is in the RPE in normal eyes but is degraded when the cells no longer phagocytose outer segments (i.e., in a macular hole). Definite identification and more precise localization of the minor fluorophore awaits further studies and detailed analyses by spectral deconvolution.

Our fluorescence measurement would not be significantly affected by either vitamin A[36] or by other components of the respiratory enzyme chain (e.g., NADH and NAD[37]) because these fluorophores are optimally excited in the 300 to 360 nm range with blue light emission. Melanin has been reported to fluoresce,[38,39] but its emission must be faint because melanin appears as dark granules in fluorescence microscopy observation of RPE. Although fluorescence of photopigment has been reported from intermediates of bleaching,[40,41] demonstration of these transient states requires low temperatures or time-resolved measurements. It is unlikely that they contribute to the fundus fluorescence reported here. Finally, Bruch's membrane has a blue–green fluorescence in fluorescence microscopy observation of RPE under ultraviolet excitations, consistent with emission spectra of collagen and elastin.[42,43] Further studies are needed to assess the influence of Bruch's membrane fluorescence on our measurements, especially in older subjects.

CONCLUSIONS

Spectral characteristics, correlation with age, topographic distribution, retinal location between the

choriocapillaris and the photoreceptors, and results from selected clinical cases provide strong evidence that the fundus fluorescence is primarily from lipofuscin and that it can be reliably measured noninvasively. Ongoing studies will further evaluate the relationship between lipofuscin and aging and will determine whether onset or progression of ARMD is significantly related to lipofuscin.

Key Words

lipofuscin, intrinsic fluorescence, autofluorescence, excitation spectrum, emission spectrum, retinal pigment epithelium, age-related macular degeneration, macular hole, Stargardt's disease

Acknowledgments

The authors thank Dr. Stephen Burns for his encouragement and advice and Dr. Frank Holz (RKU, Heidelberg, Germany) for sharing donor eyes obtained through the eyebanks of Moorefields Eye Hospital (London, England).

References

1. Feeney-Burns L, Berman ER, Rothman H. Lipofuscin of human retinal pigment epithelium. *Am J Ophthalmol.* 1980;90:783–791.
2. Boulton M, Marshall J. Effects of increasing numbers of phagocytic inclusions on human retinal pigment epithelial cells in culture: A model for aging. *Br J Ophthalmol.* 1986;70:808–815.
3. Dorey K, Staurenghi G, Delori FC. Lipofuscin in aged and ARMD eyes. In: Hollyfield JG, et al, eds. *Retinal Degeneration.* New York: Plenum Press; 1993:3–14.
4. Eldred GE. Questioning the nature of the fluorophores in age pigments. *Adv Biosci.* 1987;64:23–36.
5. Mann DMA, Yates PO. Lipoprotein pigments—their relationship to aging in the human nervous system. *Brain.* 1974;97:481–498.
6. Taylor A, Jacques PF, Dorey CK. Oxidation and aging: Impact on vision. *The International Conference on Antioxidants.* 1993;349–371.
7. Weiter JJ, Delori FC, Wing G, Fitch KA. Retinal pigment epithelial lipofuscin and melanin and choroidal melanin in human eyes. *Invest Ophthalmol Vis Sci.* 1986;27:145–152.
8. Young RW. Pathophysiology of age-related macular degeneration. *Surv Ophthalmol.* 1987;31:291–306.
9. Dorey CK, Wu G, Ebenstein D, Garsd A, Weiter JJ. Cell loss in the aging retina: Relationship to lipofuscin accumulation and macular degeneration. *Invest Ophthalmol Vis Sci.* 1989;30:1691–1699.
10. Eagle RC, Lucier AC, Bernadino VB, Janoff M. Retinal pigment epithelial abnormalities in fundus flavimaculatus: A light and electron microscopic study. *Ophthalmology.* 1980;87:1189–1200.
11. Armstrong D, Koppang N, Rider J. *Ceroid lipofuscinsosis (Battens disease).* Amsterdam: Elsevier; 1982.
12. Delori FC. Fluorophotometer for noninvasive measurement of RPE lipofuscin. *Noninvasive Assessment of the Visual System. OSA Technical Digest.* 1992;1:164–167.
13. Delori FC. Spectrophotometer for noninvasive measurement of intrinsic fluorescence and reflectance of the ocular fundus. *Applied Optics.* 1994;33:7439–7452.
14. Gass JDM. Idiopathic senile macular hole: Its early stages and pathogenesis. *Arch Ophthamol.* 1988;110:629–639.
15. ANSI. American National Standard for Safe Use of Lasers. ANSI 136.1-1993 (Revision of ANSI 136.1-1986). 1993.
16. Delori FC, Staurenghi G, Arend O, Goger DG, Weiter JJ. Estimates of ocular media absorption from fundus reflectometry. *Noninvasive Assessment of the Visual System. OSA Technical Digest.* 1994;2:220–223.
17. Wing GL, Blanchard GC, Weiter JJ. The topography and age relationship of lipofuscin concentration in the retinal pigment epithelium. *Invest Ophthalmol Vis Sci.* 1978;17:601–607.
18. Feeney-Burns L, Hilderbrand ES, Eldridge S. Aging human RPE: Morphometric analysis of macular, equatorial, and peripheral cells. *Invest Ophthalmol Vis Sci.* 1984;25:195–200.
19. Gabel V-P, Birngruber R, Hillenkamp F. Visible and near infrared light absorption in pigment epithelium and choroid. In: Shimuzu K, Osterhuis JAs, eds. *XXIII Concilium Ophthalmol Kyoto, Exerpta Medica.* Amsterdam: Oxford; 1978:658–662.
20. Delori FC, Pflibsen KP. Spectral reflectance of the human ocular fundus. *Appl Opt.* 1989;28:1061–1077.
21. van Norren D, Tiemeijer LF. Spectral reflectance of the human eye. *Vision Res.* 1986;26:313–320.
22. van Assendelft OW. *Spectroscopy of Hemoglobin Derivatives.* Springfield, IL: Charles C. Thomas; 1970:55–59.
23. Snodderly DM, Auran JD, Delori FC. The macular pigment: II: Spatial distribution in primate retinas. *Invest Ophthalmol Vis Sci.* 1984;25:674–684.
24. Elsner AE, Burns SA, Delori FC, Webb RH. Quantitative reflectometry with the SLO. In: Nasemann JE, and Burk ROs, eds. *Scanning laser ophthalmoscopy and tomography.* Munchen: Quintessenz Verlags-GmbH; 1990:109–121.
25. Liem AT, Keunen JEE, van Norren D, van der Kraats J. Rod densitometry in the aging human eye. *Invest Ophthalmol Vis Sci.* 1991;32:31–37.
26. Aaberg TM, Blair CJ, Gass JDM. Macular holes. *Am J Ophthalmol.* 1970;69:555–562.
27. Guyer D, Green WR, de Bustros S, Fine SL. Histopathologic features of idiopathic macular holes and cysts. *Ophthalmology.* 1990;97:1045–1051.
28. Pokorny J, Smith VC, Lutze M. Aging of the human lens. *Appl Opt.* 1987;26:1437–1440.
29. van Norren D, Vos JJ. Spectral transmission of the human ocular media. *Vision Res.* 1974;14:1237–1244.
30. Dorey CK, Ebenstein DB. Quantitative multispectral analysis of discrete subcellular particles by digital imaging fluorescence microscopy (DIFM). *Visual Communications and Image Processing '88 Proc Soc Photo-Optical Instr Eng.* 1988;1001:282–288.
31. Dorey CK, Ebenstein DB, Weiter JJ, Delori FC. Demonstration of multiple fluorophores within RPE lipofuscin granules by digital imaging fluorescence microscopy. ARVO Abstracts. *Invest Ophthalmol Vis Sci.* 1988;29:305.
32. Eldred GE, Katz ML. Fluorophores of the human reti-

nal pigment epithelium: Separation and spectral characterization. *Exp Eye Res.* 1988;47:71–86.

33. Eldred CE, Laskey MR. Retinal age pigments generated by self-absorbing lysosomotropic detergents. *Nature.* 1993;361:724–726.
34. Benson R, Meyer R, Zaruba M, McKhann G. Cellular autofluorescence: Is it due to flavins? *J Histochem Cytochem.* 1979;27:44–48.
35. Teich JM. *The Theory and Development of a Noninvasive Retinal Fluorescence Scanner With Application to Early Diagnosis of Diabetic Retinopathy.* Cambridge: Massachusetts Institute of Technology; 1985. PhD thesis.
36. Thomson AJ. Fluorescence spectra of some retinal polyenes. *J Chem Phys.* 1969;51:4106–4116.
37. Chance B, Schoener B, Oshino R, Itshak F, Nakase Y. Oxidation-reduction ratio studies of mitochondria in freeze-trapped samples. *J Biol Chem.* 1979;254:4764–4771.
38. Docchio F, Boulton M, Cubeddu R, Ramponi R, Dayhaw-Barker P. Age-related changes in the fluorescence of melanin and lipofuscin granules of the retinal pigment epithelium: A time-resolved fluorescence spectroscopy study. *J Photochem Photobiol.* 1991:54:247–253.
39. Fellner MJ, Chen AS, Mont M, McCabe J, Baden M. Patterns and intensity of autofluorescence and its relation to melanin in human epidermis and hair. *Int J Dermatol.* 1979;18:722–730.
40. Doukas AG, Junnarkar MR, Alfano RR, Callender RH, Kakitani T, Honig B. Fluorescence quantum yield of visual pigments: Evidence for subpicosecond isomerization rates. *Proc Natl Acad Sci USA.* 1984;81:4790–4794.
41. Guzzo AV, Pool GL. Fluorescence spectra of the intermediates of rhodopsin bleaching. *Photochem Photobiol.* 1969;9:565–570.
42. Richards-Kortum RR. Fluorescence spectroscopy as a technique for diagnosis of pathologic conditions in human arterial, urinary bladder, and gastro-intestinal tissues. Cambridge: Massachusetts Institute of Technology; 1987. PhD thesis.
43. Schomaker KT, Frisoli JK, Compton CC et al. Ultraviolet laser induced fluorescence of colonic tissue: Basic biology and diagnostic potential. *Lasers Surg Med.* 1992;12:63–78.
44. Snodderly DM, Brown PK, Delori FC, Auran JD. The macular pigment: I: Absorbance spectra, localization, and discrimination from other yellow pigments in primate retinas. *Invest Ophthalmol Vis Sci.* 1984;25:660–673.
45. Wyszecki G, Stiles WS. *Color Science: Concepts and Methods, Quantitative Data and Formulae.* New York: John Wiley & Sons; 1982:256–257.